# Performances of energy management strategies for a Photovoltaic/Battery microgrid considering battery degradation

Sarah Ouédraogo, Ghjuvan Antone Faggianelli, Guillaume Pigelet, Gilles Notton, Jean Laurent Duchaud

# Performances of energy management strategies for a Photovoltaic/Battery microgrid considering battery degradation

**Sarah Ouédraogo [1], Ghjuvan Antone Faggianelli [1]*, Guillaume Pigelet [1], Gilles Notton [1], Jean Laurent Duchaud [1]**

[1] Science for the Environment, University of Corsica, UMR CNRS 6134, 20000 Ajaccio, France.
ouedraogo_s@univ-corse.fr; pigelet_g@univ-corse.fr; notton_g@univ-corse.fr; duchaud_jl@univ-corse.fr
* Correspondence: faggianelli_ga@univ-corse.fr

**Abstract:** Several energy management strategies, of increasing complexity, are compared in term of cost benefit for a Photovoltaic /battery system providing electricity to an accommodation building with an electric vehicle. Rule based control methods with or without production forecasting are implemented and compared to a linear programming strategy used as a reference. The improvement in term of gain between simplest and reference methods is about 27%. It appears that the battery cycles number differs greatly (up to 55%), leading to a more or less rapid ageing. Battery degradation models are thus added and a corresponding cost is introduced in the strategy benefit. The results, depending on the initial battery cost, are significantly impacted, changing the relevance of the control strategies.

**Keywords:** solar microgrid; energy management system; rule based control; battery ageing model.

## 1. Introduction

The growing use of microgrids to integrate distributed energy resources (DERs) involves the use of specific controllers with integrated Energy Management Systems (EMS) for proper management and efficient system operation [1]. Such EMS can be used to schedule the operation of distributed generators (DGs), loads and storage within a microgrid, allowing the reduction of operating costs and $CO_2$ emissions. They are particularly useful when variable pricing and generation are involved [2]. We can differentiate two main types : EMS relying on mathematical optimization, using prevision of the future system behavior [3] [4], or rule based EMS consisting in a combination of rules. Rule based control (RBC) presents the advantage of being simple and easy-to-use but the rules may be hard to tune [5]. Unlike mathematical optimization such as linear or dynamic programming, they can rely or not on load and production prevision depending on their availability.

In a previous paper [6], several EMS were applied to an existing microgrid located in Ajaccio, Corsica (FRANCE). In this study, we focused on a part of the modular microgrid PAGLIA ORBA including energy production: PV modules, storage: lead acid batteries and loads: accommodation building and electric vehicle. One of the main results was to highlight the performance of a well-designed RBC in terms of cost optimization, even with multiple constraints: limitation of the power exchanged with the main grid and price fluctuation of energy (peak and off-peak hours). However, such work had a few drawbacks. At that time, only two weeks of data had been assessed. As PV production and load consumptions are affected by climate and seasonal effect, this is not enough to draw a definitive conclusion. Indeed, it seems easier to calibrate an RBC to work on a short specific period rather than on a whole year, which could be compared to the “overfitting” problem in optimization. We also observed that the different strategies had different uses of the battery reflected by various levels of SoC, DoD and cycles numbers. In these circumstances, it may be unfair not to consider the battery cost affecting the real cost of the system. This paper thus aims to overcome these two main drawbacks. For the first point, we can now provide such study with a whole year of data, allowing to test the previous RBCs on a longer period and improve them to take

seasonal effects into account. For the second point, the choice of a method to calculate battery ageing is far from trivial.

In a PV microgrid, the storage can complement variable renewable generation to improve the matching of solar PV production with electricity demand. If the PV module price decreased exponentially, the price of the energy storage also decreased importantly; between all the energy storage means, it appears clearly that for small or medium PV installations, as studied in this paper, electrochemical storage is the most appropriate. Between all the electrochemical storages, the market share of Li-ion batteries for electric vehicles (EVs) and stationary storage climbed from 5% in 2010 to more than 60 % in 2017 [7]. The Lead acid battery technology represented in 2016 about 6% of the storage market (without hydro pumping system) [8]. Even if this battery technology is today less used than Li-ion technology, it is the type of battery integrated in the PV microgrid studied in this paper. In this context, storage systems have been the subject of several researches because they represent an important part of the microgrid. Storage systems are used to stock excess energy produced by the PV plant and to supply electricity to the load when necessary; it helps balancing the grid by reducing the intermittent and random nature of renewable energy, but also supplying demand in the event of power shortage.

The utilization of battery in a PV system implies to develop methods to take a decision on its management. A storage, particularly a battery, is neither treated as production nor as load. The decision to be taken for its use depends, obviously, on the energy availability but it can also be scheduled for a future dispatch moment as per the dynamic behavior of electricity tariff, load, and production. Numerous researchers focused on optimal operating strategies of battery for increasing its performance, efficiency, and life-time [9] keeping in mind that battery is a very costly part of the microgrid. Such a strategy was developed by Tran and Khambadkone [10] with a Peukert life-time model to predict the battery life-time and a stochastic dynamic programming for optimization. They showed, in this case-study, that it is possible to improve energy efficiency of ESS from 74.1% to 85.5% (+15%) and the lifetime of two battery packs from 3.6 years to 5 years (+39%) and from 2.4 years to 5.7 years (+140 %) showing the importance of such battery management. The same Peukert model was also used to determine the loss of health for the battery which is minimized in the operation of a PV system [11]. However, Azuatalam *et al.* [12] shows that using a sophisticated EMS may not necessarily improve the performance and economic viability of the system as the battery degradation adversely affects its lifetime.

A battery life estimator with, as main variables, the varying depths and rate of discharge was considered in a power management framework for a commercial hybrid renewable microgrid with battery storage [13]. Studies on the integration of battery degradation issues within battery control are available in the literature, in which the battery defines an upper bound on the maximum number of cycles [14], or defines upper bounds and lower bounds on the state of charge of the battery without formal optimization [15].

In a multi-carrier energy hub, a cost-effective strategy based on a mixed-integer non-linear optimization and considering the degradation cost of battery were applied [16] and proved its positive impact on the economic operation of this energy hub while meeting the system's constraints. In view to extend the lifetime of the battery, the variation of the wind turbine output is reduced using an optimal dispatch strategy [17].

The degradation, life-time, operation and maintenance costs of the battery can be incorporated in the optimization process to increase the profit of a microgrid system using model predictive control (MPC) [18]. Cai *et al.* [19] also developed a MPC applied to a sustainable building in view to decrease

the utility costs while minimizing battery degradation. Bordin *et al.* [20] developed a methodology including battery degradation processes via a degradation cost inside the optimization model.

Although not exhaustive, this bibliographical study on the inclusion of battery degradation and lifetime in optimization processes for energy management highlights the importance of this topic in the development of microgrids with storage and using mainly an intermittent production from renewable sources. A literature survey on the influence of battery degradation model will be presented later.

The aim of this paper is thus to complete and improve the previous study [6] allowing to assess the relevance of using an RBC as an EMS for microgrid while taking into account the battery cost. The paper is structured as follows:

- a brief overview of the facilities (PAGLIA ORBA microgrid) and data used in this study;
- a description of the different EMS tested and their improvements;
- a presentation of the methods to consider batteries ageing cost;
- the main results considering energy and cost savings;
- the conclusion and perspectives for following works.

## 2. R&D PAGLIA ORBA microgrid

An R&D solar microgrid called PAGLIA ORBA (Figure 1) is operating in the SPE laboratory (University of Corsica, Ajaccio, FRANCE). In this study we focus on a part of this microgrid including three Distributed Generation systems (DG: 3 PV arrays of 17 kW AC), an Energy Storage System (ESS: electrochemical batteries with a total capacity of 70 kWh DC) and 2 loads (one accommodation building and one electric vehicle). This three-phase microgrid uses a common AC bus and can operate both in grid-connected or islanded mode. A general schematic is also presented in Figure 2.

*Figure 1. PAGLIA ORBA microgrid*

The PV system is composed of 3 × 56 monocrystalline silicon 327 Wp modules (SUNPOWER E20) connected to 3 x 17 kW inverters (SMA SUNNY TRIPOWER 17000TL-10). The ESS consists in 24 × 2V lead acid batteries (OPzV) in series and is operated by six inverters/chargers (STUDER INNOTEC XTENDER). For the loads, the consumption of the accommodation building varies depending on the period and the capacity of the EV is 22 kWh. The EV is used every day from 9:00 to 16:00 and is

considered as fully discharged at 16:00. From 16:00 to 18:00, the EV is charging in the microgrid with a maximum power of 22 kW and a mean power of 11 kW. If we consider the total consumption, this leads to a maximum power of 34.2 kW and a mean power of 3.5 kW.

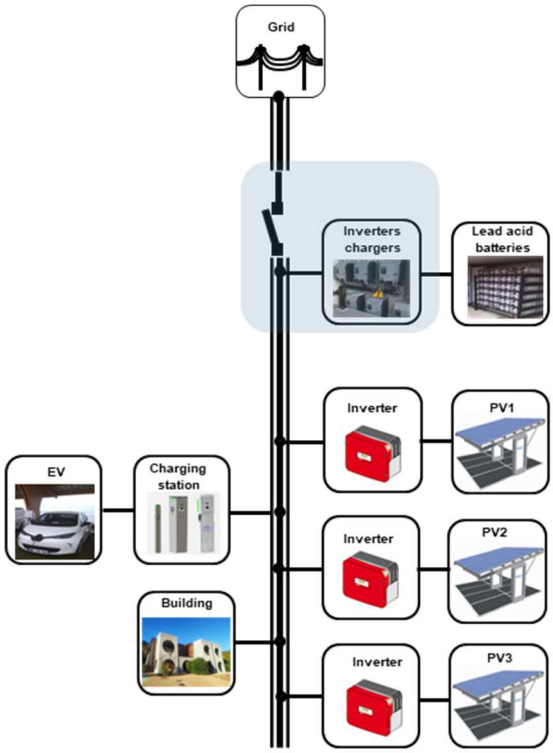


*Figure 2. General Schematic of the microgrid*

This study focuses on one year of data, from 2017 January 1st to December 31th. The daily profiles for loads and PV production for the whole period are shown in Figure 3 and Figure 4. These figures highlight the seasonal effect of PV and the variation of load consumption. Lowest values of energy consumption in summer are due to the fact that the accommodation building does not have air-conditioning. For PV profile, the treshold at 51 kW corresponds to the maximum power of the PV inverters in AC.

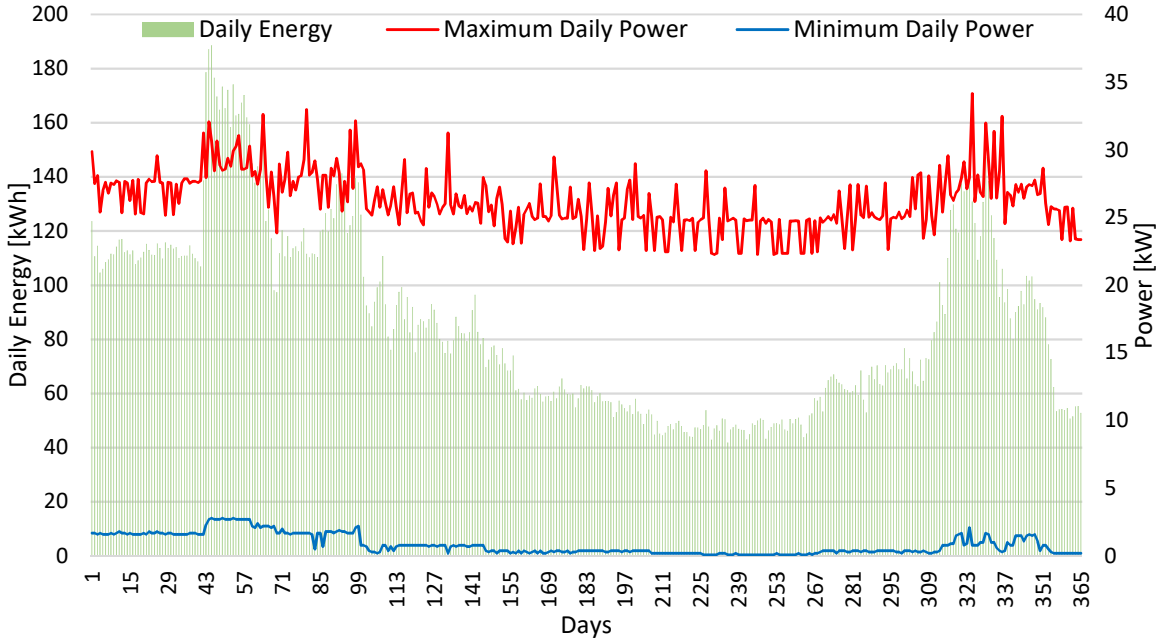


*Figure 3. Load profile*

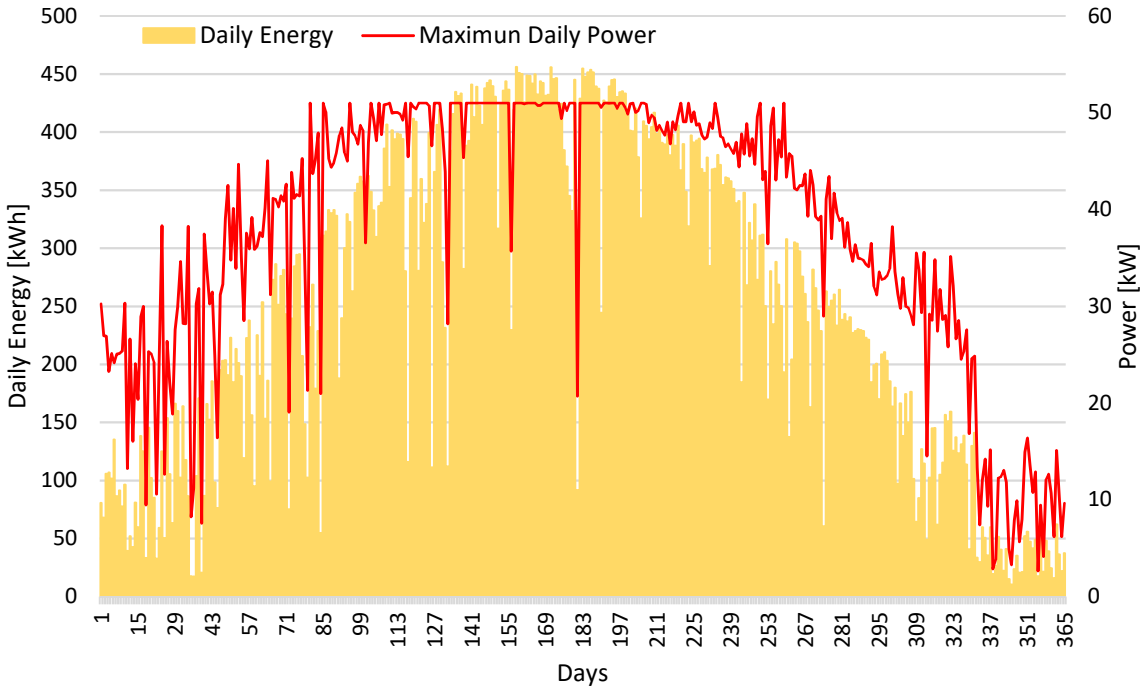


*Figure 4. PV profile (AC)*

At last, we consider that the microgrid is buying and selling energy from and to the main grid with different prices, corresponding to a real electricity contract available in this region:

- Energy bought from the main grid, $Cost_{buy}$: 122.4 €/MWh during "off-peak hours", from 22:00 to 04:00 and 163.1 €/MWh during "peak hours", from 04:00 to 22:00.
- Energy sold to the main grid, $Cost_{sell}$: constant price of 137.7 €/MWh.

## 3. EMS description

In the previous study [6], several RBC strategies had been tested and compared on a fourteen days period (March 16th to 29th). Each of them prioritizes the PV to supply the load and is based on the difference between PV and load powers:

$$\Delta = Pp - Pl \quad (1)$$

They also respect a certain number of constraints, ensuring that the repartition of the power flows is done in a realistic way. Such constraints mainly concern power limitation for PV, grid and battery as well as the battery SoC:

$$SoC_{min} \leq SoC(t) \leq SoC_{max} \quad (2)$$

$$Pp,l(t) + Pb,l(t) + Pg,l(t) + Pm(t) = Pl(t) \quad (3)$$

$$Pp,g(t) + Pb,g(t) - Pg,l(t) = Pg(t) \quad (4)$$

$$Pp,g(t) + Pp,b(t) + Pp,l(t) + Pd(t) = Pp(t) \quad (5)$$

$$0 \leq Pp,l(t) \leq Pinv^{max} \quad (6)$$

$$0 \leq Pp,g(t) \leq \min(Pg_{out}^{max}, Pinv^{max}) \quad (7)$$

$$0 \leq Pp,b(t) \leq \min\left(\frac{Pb_{in}^{max}}{\eta_{in}}, Pinv^{max}\right) \quad (8)$$

$$0 \leq Pb,l(t) \leq Pb_{out}^{max}\ \eta_{out} \quad (9)$$

$$0 \leq Pb,g(t) \leq \min(Pb_{out}^{max}\ \eta_{out}, Pg_{out}^{max}) \quad (10)$$

$$0 \leq Pg,l(t) \leq Pg_{in}^{max} \quad (11)$$

$$0 \leq Pd(t) \quad (12)$$

$$0 \leq Pm(t) \quad (13)$$

Battery admissible powers during charge and discharge are also defined by:

$$Pb_{in}^{adm} = \min\left(Pb_{in}^{max}, \frac{(1 - SoC)\ Cap_{ESS}}{dt\ \eta_{in}}\right) \quad (14)$$

$$Pb_{out}^{adm} = \max\left(-Pb_{out}^{max}, \frac{-SoC\ Cap_{ESS}\ \eta_{out}}{\mathrm{dt}}\right) \quad (15)$$

Main parameters values can be found in Table 1.

*Table 1. Parameters information*

| Parameter | Value | Description |
|---|---|---|
| $Pp^{nom}$ [kW] | 55 | PV array nominal power (DC) |
| $Pinv^{max}$ [kW] | 51 | PV inverter maximum power (AC) |
| $Pg_{out}^{max}$ [kW] | 24 | Grid maximum power output (AC) |
| $Pg_{in}^{max}$ [kW] | 24 | Grid maximum power input (AC) |
| $Cap_{ESS}$ [kWh] | 70 | Battery useful capacity (DC) |
| $Pb_{in}^{max}$ [kW] | 14 | Battery maximum power input at 0.2 C (DC) |
| $Pb_{out}^{max}$ [kW] | 35 | Battery maximum power output at 0.5 C (DC) |
| $\eta_{in}$ [-] | 0.9 | Battery charge efficiency |
| $\eta_{out}$ [-] | 0.9 | Battery discharge efficiency |

As the battery is controlled in order to prevent extreme conditions such as deep discharge and high charging/discharging current, its efficiency has been assumed to be constant and the same value is used both in charging and discharging mode [21].

At the start of the simulation, the SoC is set at 50%. At the end of the simulation it must end at 0% (battery useful capacity). This way, we can easily compare the results of all strategies. At last, the grid cannot be used to charge the battery.

Based on this information, it is possible to calculate the energy balance cost on a given period by:

$$Cost_{tot} = \sum_{t=1}^{N} \left[ Pg,l(t)\ Cost_{buy}(t) - (Pp,g(t) + Pb,g(t))\ Cost_{sell}(t) \right] dt \quad (16)$$

This cost will be the main comparison criterion for the first part of this study.

Presentation of the RBCs as well as their flowcharts are given in [6]. Here, we only propose a brief summary of these RBCs before introducing their improvement, taking into account seasonal effects.

- RBC1 is a quite simple strategy which only maximizes self-consumption. While there is enough PV power, it supplies the load and the surplus is used to charge the battery or is sold to the grid when the battery is full. When PV power is not sufficient, the missing power is supplied by the battery by priority and then by the main grid.

- In RBC2, the choice depends on the energy costs, the PV power and the battery SoC. This strategy favors the use of the grid during off-peak hours (from 22:00 to 4:00) when energy is less expensive. If a given PV level and SoC is reached, it also prevents the storage to be full too quickly by allowing the selling of PV power sooner. While reducing the self-consumption, this provides a more efficient management in terms of economy.

- RBC3 is an improvement of RBC2 considering the forecasting of the mean PV production for the next six hours. This allows the controller to manage the battery more efficiently by avoiding events such as full battery due to high PV production all over the day. This is particularly important before the sunrise, to prepare for peak hours (4:00 to 22:00) and determine the SoC level that should be kept in the battery.
  The forecasting used in this RBC is based on an Auto Regressive Mobile Average (ARMA) model [22] which has been tested in situ. By running the simulation with "perfect PV forecasting" (i.e. real data) it is also possible to calculate the maximum improvement this strategy could bring. In this case it will be referred to as RBC3r.

In order to assess the performance of the different strategies, we introduce an indicator called relative performance which indicates how close our solution is from the mathematical optimum. This optimum is obtained with a Linear Programming (LP) optimization, a mathematical optimization method for maximizing or minimizing a linear function of several variables.

The main results obtained from a 14 days' period (from [6]) and from a whole year are presented in Table 2. An interesting result is that the seasonal effects have a limited impact on RBC performances. More advanced strategies have a loss of about 4 to 5 points on relative performance, despite important changes of inputs (Figure 3). It should be noted that missing energy (around 18 kWh) now appears in all RBC and represents more than 130 shutdowns of the microgrid. Due to main

grid power limitation, the storage management has an important role for ensuring load supply. To avoid this, non-critical loads could have been switched off. However, LP results show that it is possible to manage the microgrid without any shutdown or load control. Moreover, this can even be done with fewer battery cycles, increasing the lifetime of the batteries. As mentioned in introduction, this is another important point which will be assessed later.

*Table 2. Main results comparison*

| | 14 days' period | | | | | One-year period | | | | |
|---|---|---|---|---|---|---|---|---|---|---|
| | RBC1 | RBC2 | RBC3 | RBC3r | LP | RBC1 | RBC2 | RBC3 | RBC3r | LP |
| Total gain [€] | 152.0 | 168.5 | 182.1 | 186.6 | 191.8 | 5170.3 | 5472.2 | 5896.9 | 6145.2 | 6592.7 |
| Relative performance [%] | 79.2% | 87.8% | 94.9% | 97.3% | 100% | 78.4% | 83.0% | 89.4% | 93.2% | 100% |
| Battery cycles number [-] | 13.3 | 11.5 | 11.4 | 11.5 | 6.7 | 192.7 | 218.6 | 213.3 | 208.2 | 164.1 |
| Missing energy [kWh] | 0 | 0 | 0 | 0 | 0 | 18.5 | 18.5 | 18.6 | 18.2 | 0 |

As there is still room for improvement, RBC4 introduces new rules to consider seasonal effects and compensate the missing power observed in other RBCs. Here, the operation of the microgrid changes according to two periods, extended winter and summer; winter including months from November to March, and summer months from April to October. During winter, we decide to save the battery for the peak consumption because of lower PV production. To supply the load, the system thus prioritizes the PV and then the grid, the battery being used as a security reserve in case of power shortage. During summer, we prioritize the supplying of the load by the PV production, then by the battery and finally by the grid. During this period, the PV production is high and the battery can be often full. Since the battery is frequently used, we maintain a reserve, 10% of the battery capacity, as a security to avoid missing energy. The complete flowchart of this strategy is proposed in Appendix 1.

To illustrate, one week of data are plotted for each period. Figure 5 (top) presents the results in winter where PV production is low. It can be seen that all the production is used to supply the load and the remaining share is sold to the grid, while the battery is kept at a high SoC to prevent power shortage. Figure 5 (bottom) shows the same results for a summer week. Here, we can observe the apparition of PV lost due to the battery being full early in the day. However, this phenomenon is limited by the PV forecasting, allowing the battery to be discharged in the morning.

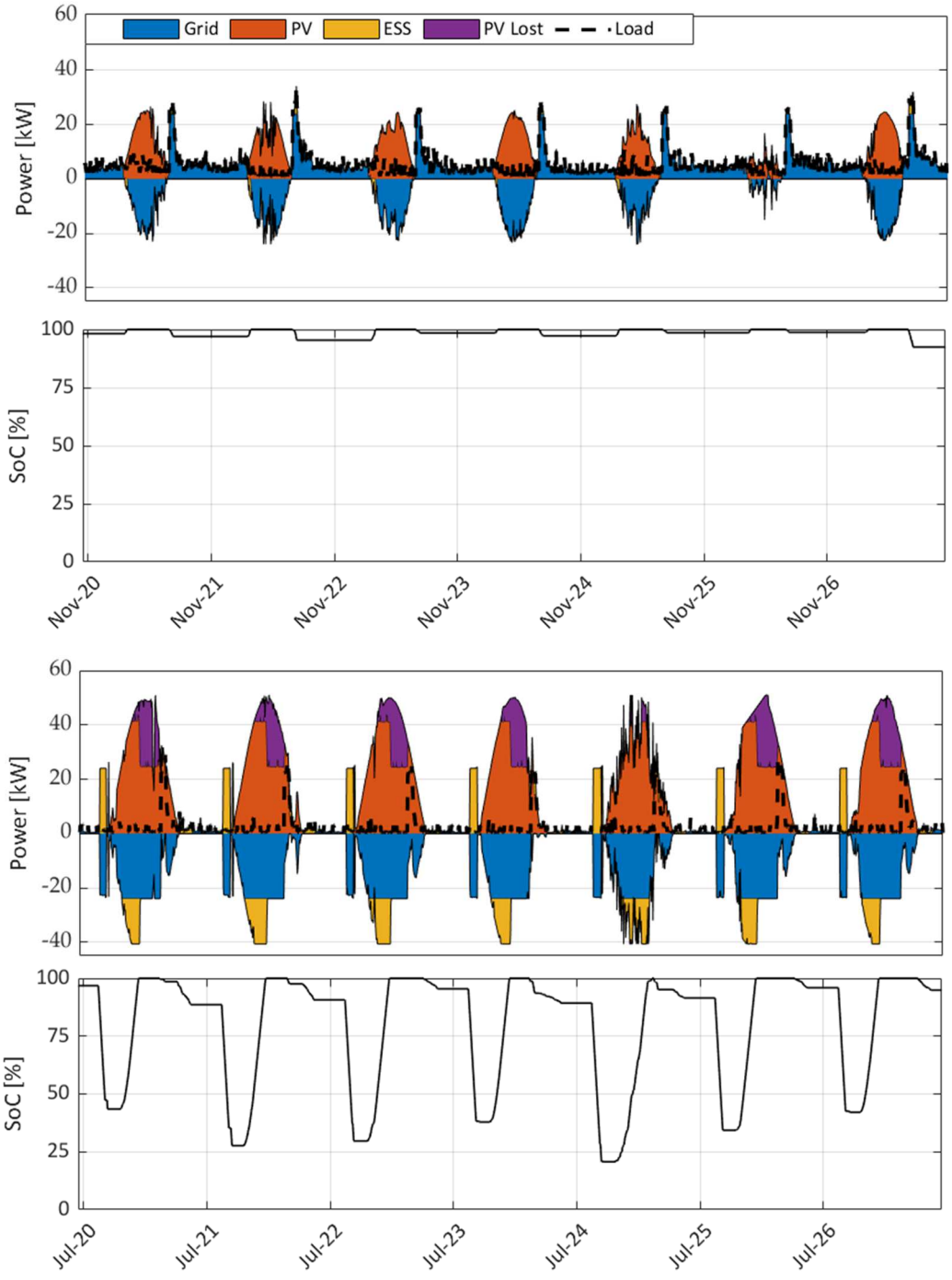


*Figure 5. RBC4r results for one week in winter (top) and summer (bottom)*

As for RBC3, the results depend on the performance of the PV forecasting model, which is not the main concern of the paper. Thus, we focus on RBC4r (perfect forecasting) showing best achievable results with a simple and realistic control strategy. These results are presented in Table 3.

*Table 3. Main results for RBC4r*

| Total gain [€] | Relative performance [%] | Battery cycles number [-] | Missing energy [kWh] |
|---|---|---|---|
| 6365.8 | 96.6% | 140.6 | 0 |

RBC4r reaches a relative performance of 96.6% for the whole year while addressing the problem of missing energy. As well as being close to LP results, it also reduces the battery use. As already shown for RBC3 and RBC3r, it should be noted that a realistic model such as ARMA will bring a loss of about 5% of the total gain. At this point, it seems more interesting to work on the load forecasting to improve these results rather than on the PV forecasting. For the next stage, we will focus on RBC4r and LP which are the only strategies optimized for a yearly period and addressing the energy missing issue, providing the same level of service.

As noted previously, according to the energy management strategy used, the number of battery cycles varies in an important range, up to 79 cycles per year (+55%), from RBC2 to RBC4r. It is obvious that the greater the cycles number is, more the battery life duration is reduced and this reduction has a cost that must be taken into account. In the next section, a short bibliographic study on battery ageing models is realized and two models will be retained to be implemented in the simulation.

## 4. Batteries ageing models

### 4.1 Bibliographic study

The behavior of a battery and the influence of various parameters (such as charge/discharge rate, voltage, temperature…) on its operation, whatever type of battery it is, is complex to understand and thus to model. Sometimes, the information found in the literature are even contradictory or at least different concerning aging effect or cycle life time, due to the fact that it is not always defined in a similar way and in the same operating conditions.

An overview of energy storage performances is given in [23] and particularly for battery storage as reported in Table 4. This clearly shows the diversity in term of performance and cost data for the same technology. These data were compiled from over 150 data sources, supplemented by expert interviews and analysis by IRENA for the latest battery developments. For calendar life, cycle life and installation cost, the reported data are worst, reference and best cases.

*Table 4. Characteristics of battery storage in 2016 [23]*

| Type | Technology | Calendar life (years) | Cycle life (equivalent full-cycle) | Installation cost (€/kWh) | Roundtrip efficiency (%) |
|---|---|---|---|---|---|
| Lead Acid | Flooded | 3-9-15 | 250-1500-2500 | 394-121-88 | 82 |
| | VR | 3-9-15 | 250-1500-2500 | 394-219-88 | 80 |
| Li-Ion | LFP | 5-12-20 | 1000-2500-10000 | 700-482-167 | 92 |
| | LTO | 10-15-20 | 5000-10000-20000 | 1051-875-394 | 96 |
| | NCA | 5-12-20 | 500-1000-2000 | 700-293-167 | 95 |
| | NMC/LMO | 5-12-20 | 500-2000-4000 | 700-350-167 | 95 |
| Redox Flow | VRFB | 5-12-20 | 12000-13000-14000 | 875-289-263 | 70 |
| | ZBFB | 5-10-20 | 300-1000-14000 | 1401-750-438 | 70 |
| High Temp | $NaNiCl_2$ | 8-15-22 | 1000-3000-7500 | 407-333-263 | 84 |
| | NaS | 10-17-25 | 1000-5000-10000 | 638-307-219 | 80 |

*VR: valve-regulated; LFP: lithium iron phosphate; LTO: lithium titanate; NCA: nickel cobalt aluminium; NCM/LMO= nickel manganese cobalt/ lithium manganese oxide; VRFB: vanadium redox flow battery; ZBFB: zinc bromine flow battery.*

As the battery has a limited lifetime, its aging can lead to significant replacement costs, so lifetime estimation is particularly important for the economic optimization of a system. As mentioned by Sauer and Wenzl [24], there are two types of aging in a battery, calendar aging and cyclic aging. Calendar aging is the degradation caused by the self-discharge of the battery. This degradation varies greatly depending on the storage conditions, which can accelerate or slow down the aging of the battery. Cyclic aging of the battery occurs when the battery is cycled (charged and discharged). In this paper, the focus is only on cyclic aging of the battery, because the batteries are considered as always used and continuously charged and discharged.

Over time, battery capacity depends on the following parameters [25]:

- the charging/discharging regime: the capacity often decreases as discharge rate increases since there is not enough time to "re-supply" the electrons through the standard chemical reaction; the Peukert's law links the battery capacity to the discharge rate [26];
- the DoD of the battery cycles during its lifetime;
- its exposure to prolonged periods of low discharge;
- the average temperature of the battery over its lifetime: the chemistry reaction rate increases with temperature; thus, an increase of the temperature has a positive influence on the capacity but also reduces the battery lifetime.

As the battery storage used in our PV/storage microgrid is lead acid battery, we focused mainly on this technology. Although lead acid batteries are an old technology, it is also a mature one *i.e.* with a large operating experience; they are still used for energy storage [27] and the research continues to improve this technology. As an example, Meyers *et al.* [28] show in their study that the addition of discrete carbon nanotubes to the positive plate increases the longevity of lead acid batteries. Another advantage of lead acid batteries are their cost, which is favorable compared to other technologies as shown in a recent paper [29].

Several types of aging models can be found in the literature. Electrochemical aging models are based on physicochemical processes that describes phenomena that affect the components (anode, cathode, electrolyte) of batteries and they require knowledge of a lot of parameters. The implementation of such a model is difficult to tackle. We must first identify the phenomena that we will need to model and those that can be neglected. Such models are detailed by Sauer and Wenzl [24]. However, due to their complexity and the need of large amount of data, this type of models cannot be used for modeling the aging of the battery in our simulation.

Other methods estimate the aging using equivalent circuits. The methods based on these models usually identify the battery by an equivalent circuit model and use different methods to estimate the parameters of these models [30]. Among them, the SimSES battery model is detailed by Naumann *et al.* [31] which is based on full cell data features, accurate loss and temperature calculation. We will not focus on this type of models either because the requested data are difficult to measure.

Bindner *et al.* [32] tested three aging lead acid battery models with specific reference to their use in hybrid renewable energy systems with wind turbine and PV systems *i.e.* with very intermittent charge and discharge rates:

- the Ah Throughput model: considering there is a fixed amount of energy that can be cycled through a battery. This calculation is done regardless of the depth of the individual cycles of the battery;
- FhG/Risø model: combining a performance model and an aging lifetime model. It models the complete power system including its control.

- UMass model: also called Kinetic Battery model, including a capacity model, a voltage model and a lifetime model.

These three models have an increasing complexity and give results in term of tested lifetime close to the experimental measures. The first one has satisfying performances and has the advantage to be easily implemented. It is also available in the HOMER software developed by NREL (National Renewable Energy Laboratory) largely used in the energy community. Haessig *et al.* [33] used this model by introducing a formulation of cycling aging based on exchanged energy counting. It fits in the ESS control optimization and allows the control to set a maximum number of battery cycles over the lifetime.

Some other simple models were developed in the literature based on the Peukert's law. Loannou *et al.* [34] determined the actual capacity of the battery used as a function of discharge current. This law was originally developed for lead acid batteries and recently extended to lithium [35]. The PLET model [36] described a relationship between the Peukert constant and the depth of discharge in lead acid battery. In this model, the capacity that the battery delivers during its lifetime is function of its depth of discharge and total number of charge/discharge cycles.

### 4.2 Description of selected models

As mentioned previously, the models must be easily implemented and must not require complex inputs to fit the need of the study. Two models were chosen: the Ah throughput model and its improvement considering the battery's depth of discharge (DoD).

- Ah Throughput Model:

As described above, this model assumes that the number of complete charge-discharge cycles that the battery can perform over its lifetime ($C_{life}$) is constant regardless of the depth of the cycles ($DoD_i$), *i.e.* two half cycles are counted as one full cycle. Here, we do not consider the SoC at the start of the cycle and at the end of the cycle, but only the cycle amplitude. The number of full cycles that the battery performs ($C_{rea}$) is equal to the sum of the depth of each cycle ($DoD_i$):

$$C_{rea} = \sum_{i=1}^{N} DoD_i \tag{17}$$

We used the number of cycles to quantify the degradation ratio $A$ at the end of the simulation:

$$A = \frac{C_{rea}}{C_{life}} \tag{18}$$

When $A$ reaches 1, the battery is at the end of its life.

In this model we took $C_{life} = 1200$ full cycles. This number has been obtained by interpolating the OPzV battery discharge curve described by the manufacturer [37]. It is close to the reference value presented in Table 4.

- Degradation model depending on the DoD:

This model is an improvement of the Ah Throughput model. In this model, the number of full cycles that the battery can perform over its lifetime varies with the depth of each cycle. Thus,

considering each cycle $i$ of $DoD_i$ we know the number of cycles achievable over the life of the battery ($C_{life,i}$). Here, we also use the data from the OPzV battery discharge curve given by the manufacturer [37] (Figure 6).

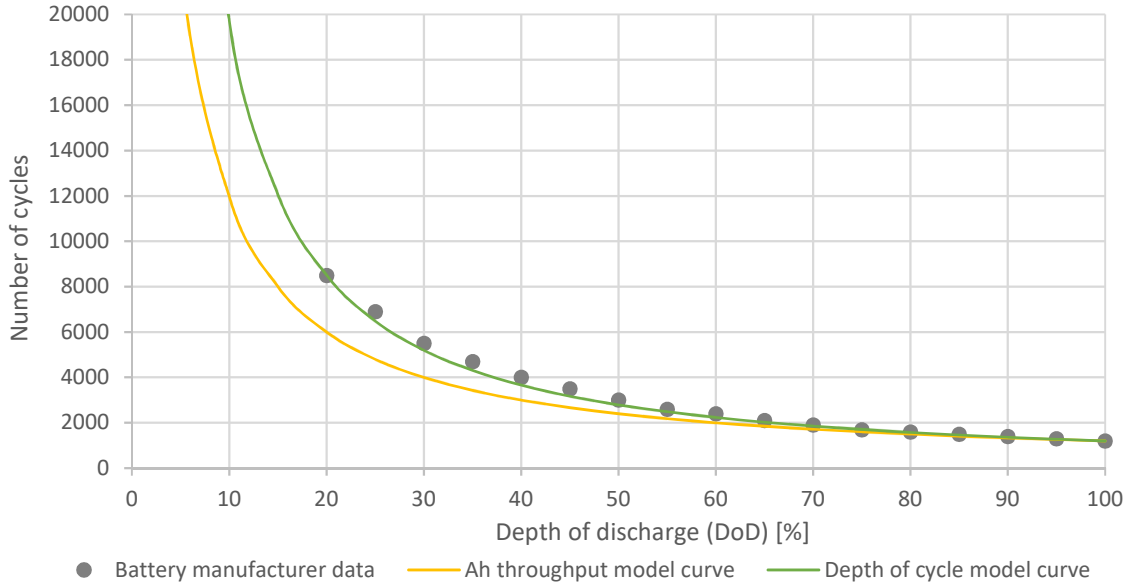


*Figure 6. Battery cycles curves*

Compared with the first model, there is a higher increase in $C_{life,i}$ when the DoD of the cycles decreases. To model the number of cycles according to the DoD of each cycle $i$, a linear, exponential, polynomial or power function can be used [38]. A power function, represented by green curve in Figure 6, is used:

$$C_{life,i} = 325000 * (DoD_i * 100)^{-1.2162} \tag{19}$$

In this model, we have to recalculate the equivalent $DoD_{i,eq}$ for each cycle $i$:

$$DoD_{eq,i} = \frac{C_{life}}{C_{life,i}} \tag{20}$$

And then $C_{rea}$ is calculated as the sum of $DoD_{eq,i}$:

$$C_{rea} = \sum_{i=1}^{N} DoD_{eq,i} \tag{21}$$

## 5. Models implementation in simulation

Battery ageing models can be implemented both at the end of the simulation or at each time step of the simulation. In this study, the two methods have been tested. The first one provides an estimation of the real cost for the proposed strategies while the second one allows the use of this information in the decision process.

### 5.1 At the end of the simulation

To use both models at the end of the simulation, the $DoD_i$ of each cycle is calculated at the end by the rainflow cycle counting algorithm [39]. This algorithm is used to study fatigue, to decompose the cycles performed by the battery, using the extremums of the cycles. It takes as input the SoC of the battery and identifies the amplitude of all the cycles contained in the series.

### 5.2 During the simulation

To optimize the energy management in the microgrid considering the aging of the battery in the decision parameters, it is necessary to have a continuous cycle counting. Here, it is not possible to use a rainflow algorithm for continuous cycle counting. Instead, a dynamic cycle counting is used. This model also used by Haessig *et al.* [33] allows the knowledge of the instantaneous degradation of the battery.

The degradation value $A_i(t)$ at each time step is calculated using the battery requirement represented by the DoD variation and the battery lifetime. At the beginning of a new cycle $i$, it is calculated as:

$$A_i(t) = \frac{|DoD_i(t) - DoD_i(t-1)|}{C_{life,i}(t)} \tag{22}$$

Then during a cycle $i$, the degradation increases according to:

$$A_i(t) = A_i(t-1) + \frac{|DoD_i(t) - DoD_i(t-1)|}{C_{life,i}(t)} \tag{23}$$

### 5.3 Degradation pricing

The degradation is priced by assuming that the batteries will have to be replaced when $A$ reaches 1. The battery installation cost $R$ must be adjusted according to the estimation of the batteries price. In this study, we use the cost range proposed by IRENA in Table 4 [23] for lead acid technology (from about 100 to 400 €/kWh).

The cost of the degradation ($Cost_{bat}$) is then calculated at the end of the simulation:

$$Cost_{bat} = A * R \tag{24}$$

Or at each timestep:

$$Cost_{bat}(t) = A_i(t) * R \tag{25}$$

At last, to take into account the degradation cost in the battery management, it can be added to the objective function:

$$Cost_{tot} = \sum_{t=1}^{N} \left[ Pg,l(t) Cost_{buy}(t) + Pb * Cost_{bat}(t) - \left( Pp,g(t) + Pb,g(t) \right) Cost_{sell}(t) \right] dt \tag{26}$$

For RBCs, a condition must be added in the decision process. The battery degradation cost has thus been implemented in RBC4r. $Cost_{bat}(t)$ is compared to the electricity purchase tariff $Cost_{buy}(t)$ in case of load demand and when $Cost_{bat}(t) < Cost_{buy}(t)$ battery can be used to supply the load, otherwise the grid is used. In the situation where the grid cannot supply the whole load, the battery is used without considering the cost of degradation in order to avoid missing energy. To avoid any confusion, this strategy will be called RBC5r.

## 5.4 Simulation results

In this section, the two battery degradation models described previously are tested for the two optimized strategies: RBC4r and LP. To begin, they are applied at the end of the simulation to estimate the real cost of these strategies. Table 5 introduces the battery degradation ratio ($A$) while the Figure 7 presents the total gain including the battery cost.

*Table 5. Battery degradation results for the two models*

| | RBC4r | LP |
|---|---|---|
| Battery degradation (Ah Throughput) [%] | 11.68 | 14.04 |
| Battery degradation (depending on DoD) [%] | 10.79 | 12.02 |

As expected, the Ah Throughput model induces a higher degradation due to the linear counting method. However, it is not so different from its improvement taking into account the battery DoD. It seems still interesting to use it if we want to keep a safety margin in order to avoid overestimating the gain. As the degradation is calculated as a percentage, this difference will greatly increase with the battery cost. The greater the battery cost, the more impact the choice of the model will have.

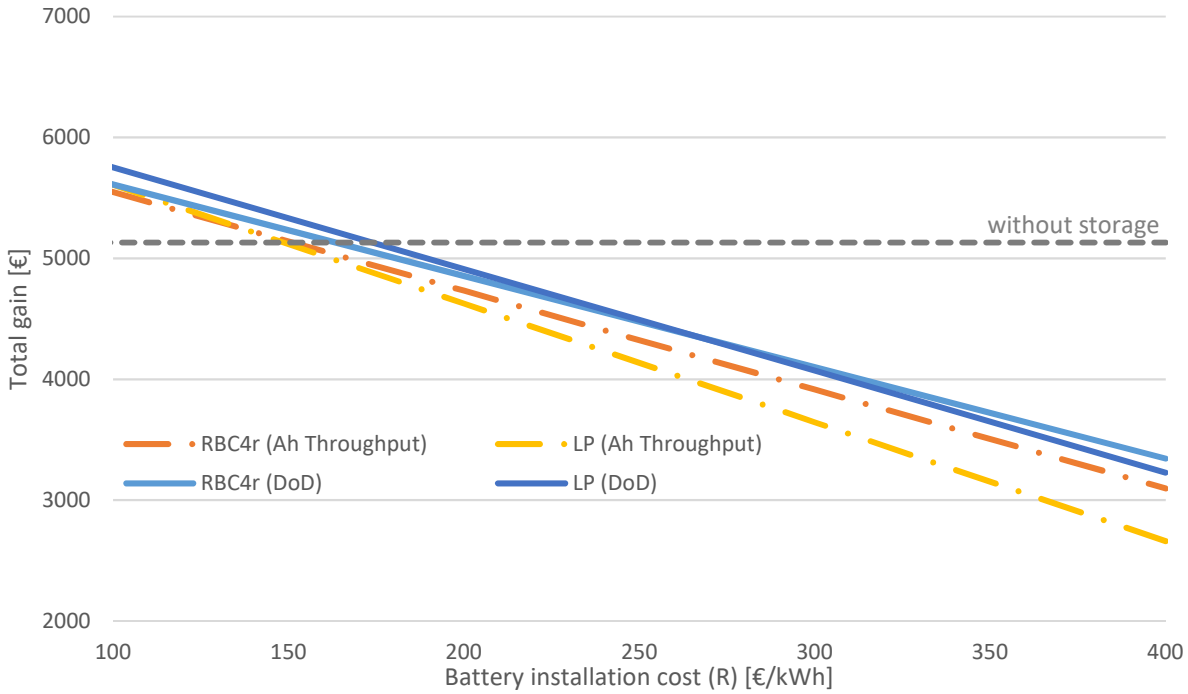


*Figure 7. Total gain for different battery installation costs*

Figure 7 presents the total gain for different battery installation costs. It also includes the total gain without storage to highlight the battery cost from which the battery improves the profitability of the system. Depending on the battery degradation model and the strategy, this cost varies between 150 and 175 €/kWh which is close to the average value from IRENA estimation (Table 4). Below this threshold, the battery is still important as it provides an efficient way to tackle missing energy and allows the increase of PV share in the microgrid.

These results confirm the importance of considering the battery cost in the strategy used. To go further, we compare the benefit with the consideration of battery degradation as a decision parameter during simulation. For RBC5r, both degradation models can be used for continuous cycle counting. However, the model depending on DoD introduces non-linearity and will not be tested with the LP.

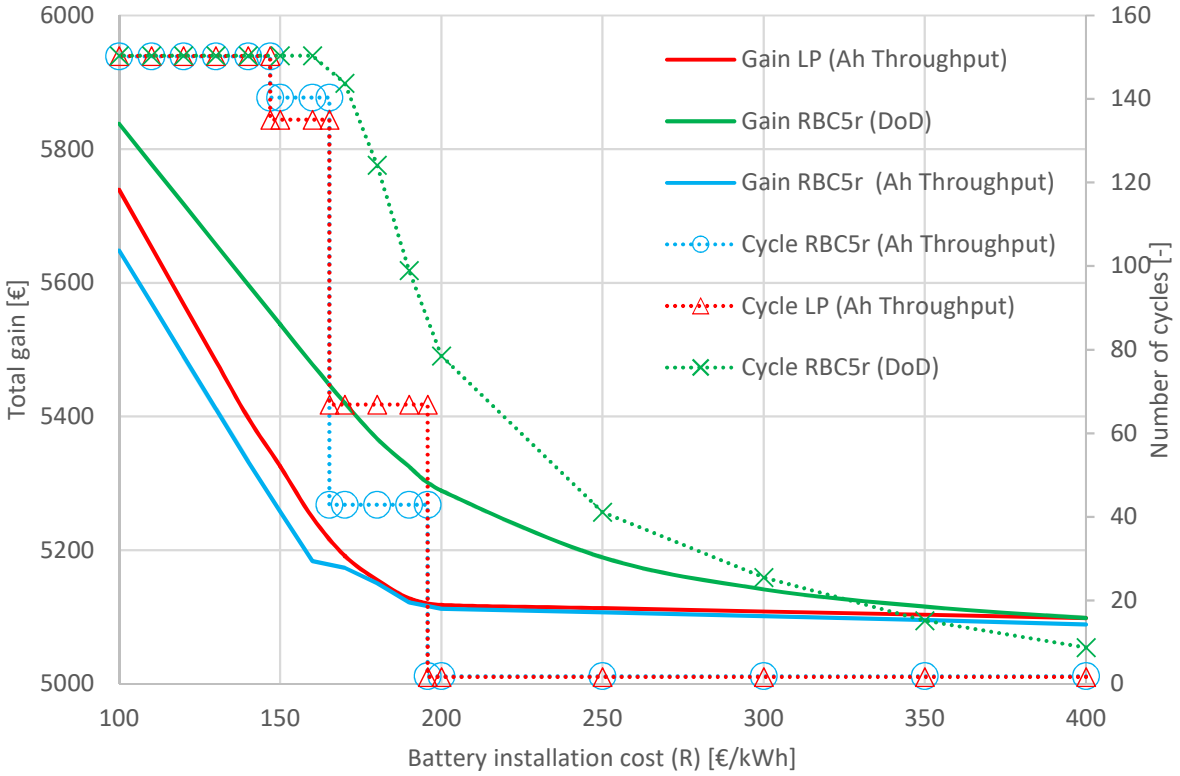


*Figure 8. Total gain and number of cycles depending on battery cost and degradation model*

The total gain as well as number of cycles depending on battery costs and degradation models are presented in Figure 8. With the Ah Throughput model, we observe that from to 200 to 100 €/kWh the battery usage increases significantly. In this range, the number of cycles presents three plateaux corresponding to threshold values where battery costs became profitable compared respectively with peak hours electricity tariff, grid electricity selling price and off-peak hours electricity tariff. From 200 €/kWh, the battery is only used to avoid missing energy, which represent about two cycles. In this case, it should be noted that the storage sizing may be no more reliable as a smaller battery capacity would be less expensive and sufficient to compensate missing energy. Comparing RBC5r to LP, it can be seen that both methods give similar results with a battery cost of more than 170 €/kWh. The difference below this value is not so significant and shows that a well-designed RBC can be suitable to manage the system. With the model depending on DoD, which is more realistic, we observe that the battery is still used even at higher costs. For low battery costs (less than 150 €/kWh), the number of cycles converged and the only difference concerns the total gain.

## 6. Conclusion

Several strategies of energy management were developed and compared: the complexity of the management algorithm is increased from a simple self-consumption strategy to a linear programming optimization used as a reference. These strategies are rule based control algorithms considering the sold and purchased kWh tariff and a forecasting of the photovoltaic production.

The simulations are applied to a PV/battery system integrated into a smart microgrid supplying a small accommodation building and an electric vehicle on a yearly basis. For each strategy, several variables were computed: energy produced by the PV system or lost when the storage is full, non-satisfied load energy, electrical grid energy, number of battery cycles…

The sold and purchased electricity cost is calculated leading to a total gain, the best strategy being considered as the most “profitable”. The cost of the production system, which is the same for all cases, is not taken into account because only the influence of the energy management is studied.

The variation of the load and the PV production over the year conduced us to develop a seasonal strategy with two periods (RBC4) with different rules for both seasons; this strategy showed an interesting improvement. It appeared that according to the strategy used, the total gain varies greatly, between 5170 € per year for RBC1 to 6366 € (+ 23%) and 6593 € (+ 27%) for RBC4r and LP. However, it was noted that the number of battery cycles is different, varying from 141 cycles to 219 cycles per year (+ 55%). This variation induces a more or less fast ageing and a more or less frequent replacement that needs to be considered in the cost balance.

A bibliographical study showed that several ageing battery models exist in the literature with different degrees of complexity and various input parameters often difficult to obtain and to implement. Two models were retained, the Ah throughput model and its improvement considering the battery DoD. Both have been implemented to calculate the cost at the end of the simulation as well as at each timestep, in the decision process.

With the inclusion of the battery degradation cost, the results are very different to the previous ones confirming the necessity to introduce this factor in the simulation. It appears immediately that considering the battery ageing has for consequences to make its utilization less frequent, depending on the battery installation cost. The use of a battery storage in such a system integrated in a smart microgrid is economically cost-effective only if the battery installation cost does not exceed a certain threshold (about 150 €/kWh) which is today an average value for lead acid battery in the market. However, whatever the price of the battery is, its presence allows the removal of the non-satisfied load energy and the increase of the green energy share in the system energy balance.

In this work, the optimization has been done on the balance cost of electricity but other ones can be added such as the environmental quality of the electricity, favouring the electricity supplied by the PV system instead of the one provided by the main grid, often with higher carbon footprint.

Various perspectives are open:

- The study of the PV and battery size influence on the strategy performances.
- A more developed cost study considering the total investment cost of the system, O&M and replacement cost on the system life duration.
- A study on the impact of the sold and purchased electricity tariff with a variation over the time, more adapted to a smart management of renewable energy production.
- The coupling of these strategies with a power management system to test them in real-time on PAGLIA ORBA microgrid.

## *Nomenclature*

| Symbol | Description | Unit |
|---|---|---|
| ARMA | Auto Regressive Mobile Average | |
| DG | Distributed Generation | |
| DoD | Depth of Discharge | |
| ESS | Energy Storage System | |
| EMS | Energy Management System | |
| EV | Electric Vehicle | |
| LP | Linear Programming | |
| MPC | Model Predictive Control | |
| PV | Photovoltaic | |
| RBC | Rule Based Control | |
| SoC | State of Charge | |
| $A$ | Degradation ratio | [-] |
| $C_{life}$ | Maximum number of full battery cycles | [-] |
| $C_{rea}$ | Effective number of full battery cycles | [-] |
| $Cap_{ESS}$ | Battery useful capacity | [kWh] |
| $Cost_{buy}$ | Energy buying price | [€/kWh] |
| $Cost_{sell}$ | Energy selling price | [€/kWh] |
| $Cost_{tot}$ | Energy balance cost | [€] |
| $dt$ | Time step | [min] |
| $Pp$ | PV power | [kW] |
| $Pl$ | Load power | [kW] |
| $Pg$ | Grid power | [kW] |
| $Pd$ | Degraded PV power | [kW] |
| $Pm$ | Missing power | [kW] |
| $Pp,l$ | PV power to load | [kW] |
| $Pp,b$ | PV power to battery | [kW] |
| $Pp,g$ | PV power to grid | [kW] |
| $Pb,l$ | Battery power to load | [kW] |
| $Pb,g$ | Battery power to grid | [kW] |
| $Pg,l$ | Grid power to load | [kW] |
| $Pp^{nom}$ | PV array nominal power | [kW] |
| $Pinv^{max}$ | Inverter maximum power | [kW] |
| $Pg_{out}^{max}$ | Grid maximum power output | [kW] |
| $Pg_{in}^{max}$ | Grid maximum power input | [kW] |
| $Pb_{in}^{max}$ | Battery maximum power input | [kW] |
| $Pb_{out}^{max}$ | Battery maximum power output | [kW] |
| $Pb_{in}^{adm}$ | Battery admissible power input | [kW] |
| $Pb_{out}^{adm}$ | Battery admissible power output | [kW] |
| $R$ | Battery installation cost | [€] |
| $\Delta$ | Difference between PV power and Load power | [kW] |
| $\eta_{in}$ | Battery charge efficiency | [-] |
| $\eta_{out}$ | Battery discharge efficiency | [-] |

## *References*


[1] M. Restrepo, C. A. Cañizares, J. W. Simpson-Porco, P. Su, and J. Taruc, 'Optimization- and Rule-based Energy Management Systems at the Canadian Renewable Energy Laboratory microgrid facility', *Applied Energy*, vol. 290, p. 116760, May 2021, doi: 10.1016/j.apenergy.2021.116760.

[2] Y. Ozturk, D. Senthilkumar, S. Kumar, and G. Lee, 'An Intelligent Home Energy Management System to Improve Demand Response', *IEEE Transactions on Smart Grid*, vol. 4, no. 2, pp. 694–701, Jun. 2013, doi: 10.1109/TSG.2012.2235088.

[3] D. E. Olivares, C. A. Cañizares, and M. Kazerani, 'A Centralized Energy Management System for Isolated Microgrids', *IEEE Transactions on Smart Grid*, vol. 5, no. 4, pp. 1864–1875, Jul. 2014, doi: 10.1109/TSG.2013.2294187.

[4] W. C. Clarke, M. J. Brear, and C. Manzie, 'Control of an isolated microgrid using hierarchical economic model predictive control', *Applied Energy*, vol. 280, p. 115960, Dec. 2020, doi: 10.1016/j.apenergy.2020.115960.

[5] Y. Zhu, Y. Chen, G. Tian, H. Wu, and Q. Chen, 'A four-step method to design an energy management strategy for hybrid vehicles', in *Proceedings of the 2004 American control conference*, 2004, vol. 1, pp. 156–161.

[6] S. Ouédraogo, G. A. Faggianelli, G. Pigelet, J. L. Duchaud, and G. Notton, 'Application of Optimal Energy Management Strategies for a Building Powered by PV/Battery System in Corsica Island', *Energies*, vol. 13, no. 17, p. 4510, Jan. 2020, doi: 10.3390/en13174510.

[7] N. Kittner, O. Schmidt, I. Staffell, and D. M. Kammen, 'Chapter 8 - Grid-scale energy storage', in *Technological Learning in the Transition to a Low-Carbon Energy System*, M. Junginger and A. Louwen, Eds. Academic Press, 2020, pp. 119–143. doi: 10.1016/B978-0-12-818762-3.00008-X.

[8] IEA, 'Tracking Clean Energy Progress 2017 – Analysis', IEA, Paris, May 2017. Accessed: Jun. 10, 2021. [Online]. Available: https://www.iea.org/reports/tracking-clean-energy-progress-2017

[9] N. K. Paliwal, 'A day-ahead Optimal Scheduling Operation of Battery Energy Storage with Constraints in Hybrid Power System', *Procedia Computer Science*, vol. 167, pp. 2140–2152, 2020, doi: 10.1016/j.procs.2020.03.263.

[10] D. Tran and A. M. Khambadkone, 'Energy Management for Lifetime Extension of Energy Storage System in Micro-Grid Applications', *IEEE Transactions on Smart Grid*, vol. 4, no. 3, pp. 1289–1296, Sep. 2013, doi: 10.1109/TSG.2013.2272835.

[11] Y. Qin, H. Hua, and J. Cao, 'Stochastic Optimal Control Scheme for Battery Lifetime Extension in Islanded Microgrid via a Novel Modeling Approach', *IEEE Transactions on Smart Grid*, vol. 10, no. 4, pp. 4467–4475, Jul. 2019, doi: 10.1109/TSG.2018.2861221.

[12] D. Azuatalam, K. Paridari, Y. Ma, M. Förstl, A. C. Chapman, and G. Verbič, 'Energy management of small-scale PV-battery systems: A systematic review considering practical implementation, computational requirements, quality of input data and battery degradation', *Renewable and Sustainable Energy Reviews*, vol. 112, pp. 555–570, Sep. 2019, doi: 10.1016/j.rser.2019.06.007.

[13] S. A. Pourmousavi, R. K. Sharma, and B. Asghari, 'A framework for real-time power management of a grid-tied microgrid to extend battery lifetime and reduce cost of energy', in *2012 IEEE PES Innovative Smart Grid Technologies (ISGT)*, Washington, DC, Jan. 2012, pp. 1–8. doi: 10.1109/ISGT.2012.6175707.

[14] S. Kato, H. Nishihara, I. Taniguchi, M. Fukui, and K. Sakakibara, 'Analysis on battery storage utilization in decentralized solar energy networks based on a mathematical programming model', in *The 6th International Conference on Soft Computing and Intelligent Systems, and The 13th International Symposium on Advanced Intelligence Systems*, Nov. 2012, pp. 651–656. doi: 10.1109/SCIS-ISIS.2012.6505251.

[15] R. Patil and R. Sharma, 'Quantifying the impact of battery constraints on microgrid operation using optimal control', in *ISGT 2014*, Feb. 2014, pp. 1–5. doi: 10.1109/ISGT.2014.6816419.

[16] M. S. Javadi, A. Anvari-Moghaddam, and J. M. Guerrero, 'Optimal scheduling of a multi-carrier energy hub supplemented by battery energy storage systems', in *2017 IEEE International Conference on Environment and Electrical Engineering and 2017 IEEE Industrial and Commercial*

*Power Systems Europe (EEEIC / I CPS Europe)*, Jun. 2017, pp. 1–6. doi: 10.1109/EEEIC.2017.7977520.

[17] F. Luo, K. Meng, Z. Y. Dong, Y. Zheng, Y. Chen, and K. P. Wong, 'Coordinated Operational Planning for Wind Farm With Battery Energy Storage System', *IEEE Transactions on Sustainable Energy*, vol. 6, no. 1, pp. 253–262, Jan. 2015, doi: 10.1109/TSTE.2014.2367550.

[18] F. García and C. Bordons, 'Optimal economic dispatch for renewable energy microgrids with hybrid storage using Model Predictive Control', in *IECON 2013 - 39th Annual Conference of the IEEE Industrial Electronics Society*, Nov. 2013, pp. 7932–7937. doi: 10.1109/IECON.2013.6700458.

[19] J. Cai, H. Zhang, and X. Jin, 'Aging-aware predictive control of PV-battery assets in buildings', *Applied Energy*, vol. 236, pp. 478–488, Feb. 2019, doi: 10.1016/j.apenergy.2018.12.003.

[20] C. Bordin, H. O. Anuta, A. Crossland, I. L. Gutierrez, C. J. Dent, and D. Vigo, 'A linear programming approach for battery degradation analysis and optimization in offgrid power systems with solar energy integration', *Renewable Energy*, vol. 101, pp. 417–430, Feb. 2017, doi: 10.1016/j.renene.2016.08.066.

[21] A. Parisio, E. Rikos, G. Tzamalis, and L. Glielmo, 'Use of model predictive control for experimental microgrid optimization', *Applied Energy*, vol. 115, pp. 37–46, Feb. 2014, doi: 10.1016/j.apenergy.2013.10.027.

[22] J. G. De Gooijer and R. J. Hyndman, '25 years of time series forecasting', *International Journal of Forecasting*, vol. 22, no. 3, pp. 443–473, Jan. 2006, doi: 10.1016/j.ijforecast.2006.01.001.

[23] IRENA, 'Electricity Storage and Renewables: Costs and Markets to 2030', International Renewable Energy Agency, Abu Dhabi, 2017.

[24] D. U. Sauer and H. Wenzl, 'Comparison of different approaches for lifetime prediction of electrochemical systems—Using lead-acid batteries as example', *Journal of Power Sources*, vol. 176, no. 2, pp. 534–546, Feb. 2008, doi: 10.1016/j.jpowsour.2007.08.057.

[25] A. J. Ruddell *et al.*, 'Analysis of battery current microcycles in autonomous renewable energy systems', *Journal of Power Sources*, vol. 112, no. 2, pp. 531–546, Nov. 2002, doi: 10.1016/S0378-7753(02)00457-3.

[26] D. Doerffel and S. A. Sharkh, 'A critical review of using the Peukert equation for determining the remaining capacity of lead-acid and lithium-ion batteries', *Journal of Power Sources*, vol. 155, no. 2, pp. 395–400, Apr. 2006, doi: 10.1016/j.jpowsour.2005.04.030.

[27] 'ITRI-Report-Tin-in-Lead-Acid-Batteries-260318.pdf'. Accessed: Jun. 10, 2021. [Online]. Available: https://www.internationaltin.org/wp-content/uploads/2018/03/ITRI-Report-Tin-in-Lead-Acid-Batteries-260318.pdf

[28] J. P. Meyers *et al.*, 'Discrete carbon nanotubes promote resistance to corrosion in lead-acid batteries by altering the grid-active material interface', *Journal of Energy Storage*, vol. 32, p. 101983, Dec. 2020, doi: 10.1016/j.est.2020.101983.

[29] G. J. May, A. Davidson, and B. Monahov, 'Lead batteries for utility energy storage: A review', *Journal of Energy Storage*, vol. 15, pp. 145–157, Feb. 2018, doi: 10.1016/j.est.2017.11.008.

[30] M. Einhorn, F. V. Conte, C. Kral, J. Fleig, and R. Permann, *Parameterization of an electrical battery model for dynamic system simulation in electric vehicles*. 2010, p. 7. doi: 10.1109/VPPC.2010.5729127.

[31] M. Naumann, C. N. Truong, M. Schimpe, D. Kucevic, A. Jossen, and H. C. Hesse, 'SimSES: Software for techno-economic Simulation of Stationary Energy Storage Systems', in *International ETG Congress 2017*, Nov. 2017, pp. 1–6.

[32] H. Bindner, T. Cronin, P. Lundsager, J. Manwell, U. Abdulwahid, and I. Baring-Gould, 'Lifetime Modelling of Lead Acid Batteries', Jan. 2005.

[33] P. Haessig, H. BEN AHMED, and B. Multon, 'Energy Storage Control with Aging Limitation', Eindhoven, Netherlands, Jun. 2015. doi: 10.1109/PTC.2015.7232683.

[34] D. Doerffel and S. A. Sharkh, 'A critical review of using the Peukert equation for determining the remaining capacity of lead-acid and lithium-ion batteries', *Journal of Power Sources*, vol. 155, no. 2, pp. 395–400, Apr. 2006, doi: 10.1016/j.jpowsour.2005.04.030.

570 [35] N. Omar, P. V. den Bossche, T. Coosemans, and J. V. Mierlo, 'Peukert Revisited—Critical
571 Appraisal and Need for Modification for Lithium-Ion Batteries', *Energies*, vol. 6, no. 11, pp.
572 5625–5641, Nov. 2013, doi: 10.3390/en6115625.
573 [36] D. Tran and A. M. Khambadkone, 'Energy Management for Lifetime Extension of Energy Storage
574 System in Micro-Grid Applications', *IEEE Transactions on Smart Grid*, vol. 4, no. 3, pp. 1289–
575 1296, Sep. 2013, doi: 10.1109/TSG.2013.2272835.
576 [37] HOPPECKE, 'Installation, commissioning and operating instructionsfor valve-regulated
577 stationary lead-acid batteries', 7140203153 V1.4 (, 2021. [Online]. Available:
578 https://www.hoppecke.com/fileadmin/Redakteur/Hoppecke-Main/Products-
579 Import/vrl_manual_en.pdf
580 [38] B. Xu, A. Oudalov, A. Ulbig, G. Andersson, and D. S. Kirschen, 'Modeling of Lithium-Ion Battery
581 Degradation for Cell Life Assessment', *IEEE Transactions on Smart Grid*, vol. 9, no. 2, pp. 1131–
582 1140, Mar. 2018, doi: 10.1109/TSG.2016.2578950.
583 [39] S. D. Downing and D. F. Socie, 'Simple rainflow counting algorithms', *International Journal of*
584 *Fatigue*, vol. 4, no. 1, pp. 31–40, Jan. 1982, doi: 10.1016/0142-1123(82)90018-4.
585

*Appendix 1. RBC4 flowchart*